

Supplementary Data

Stabilization of Lithium Metal Anodes by Conductive Metal-Organic Framework Architectures

Jing Zhao,^{ab} Hongye Yuan,^a Guiling Wang,^{*b} Xiao Feng Lim,^a Hualin Ye,^a Vanessa Wee,^a Yongzheng Fang,^b Jim Yang Lee,^{*a} Dan Zhao,^{*a}

^a Department of Chemical and Biomolecular Engineering, National University of Singapore, Singapore 117585, Singapore

^b Key Laboratory of Superlight Materials and Surface Technology of Ministry of Education, Department of Materials Science and Engineering, Harbin Engineering University, Harbin, Heilongjiang, 150001, P. R. China

Corresponding Author

^{a,*} Dan Zhao E-mail: chezhao@nus.edu.sg, Jim Yang Lee E-mail: cheleejy@nus.edu.sg.

^{b,*} Guiling Wang E-mail: wangguiling@hrbeu.edu.cn.

Table of Contents

1. Supplementary Table.....	S3
2. Supplementary Figures.....	S4

1. Supplementary Table

Table S1. The values of adsorption energy and diffusion barrier of Li ions on different surfaces calculated by the DFT method.

Sample	Adsorption energy (eV Å ⁻²)	Diffusion barrier (eV Å ⁻²)
Cu (111)	-2.37	1.76
Ni ₃ (HITP) ₂ @Cu-foil	-3.18	0.71

2. Supplementary Figures

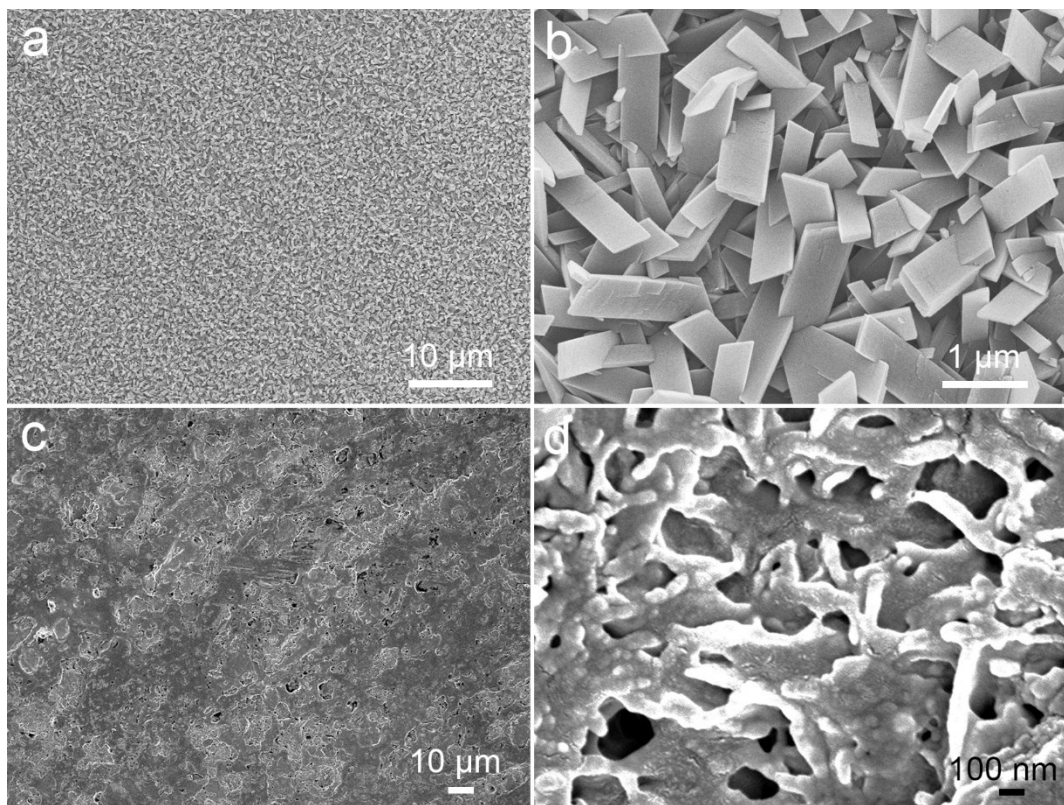


Fig. S1. SEM images of Ni-NDC@Cu-foil current collector: (a) low magnification, (b) high magnification. SEM images of Ni₃(HITP)₂@Cu-foil after cycling: (c) low magnification, (d) high magnification.

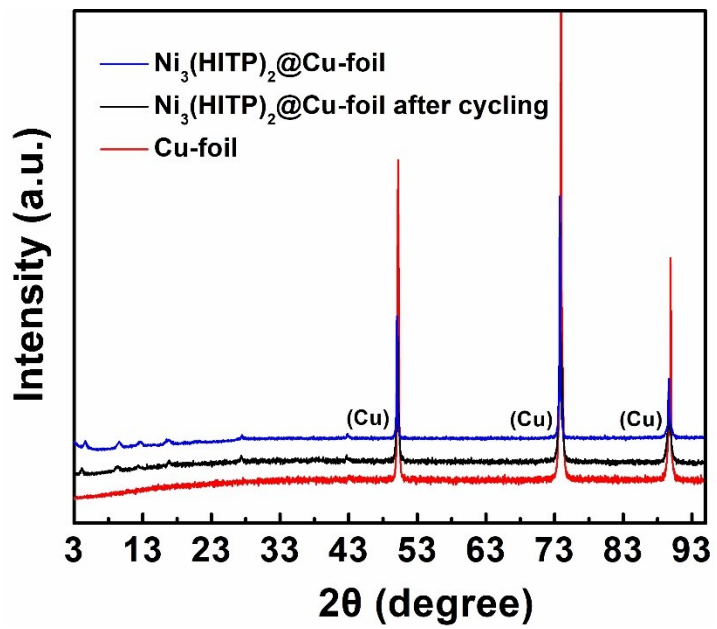


Fig. S2. Full XRD patterns of different current collectors.

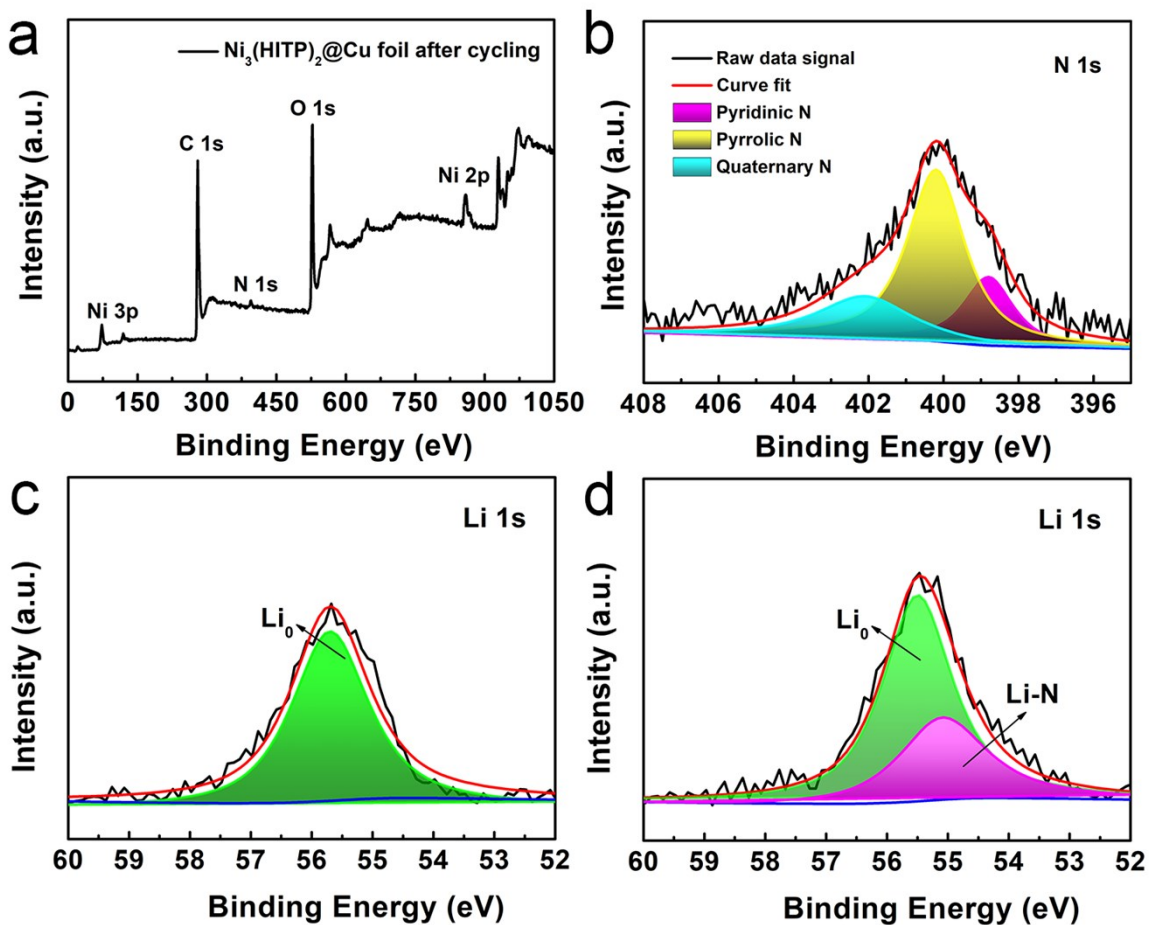


Fig. S3. (a) Wide-scan XPS spectra and (b) high-resolution N 1s XPS spectra of the $\text{Ni}_3(\text{HITP})_2@\text{Cu}$ -foil after cycling. Li 1s XPS spectra of (c) initial $\text{Ni}_3(\text{HITP})_2@\text{Cu}$ -foil and (d) Li/ $\text{Ni}_3(\text{HITP})_2@\text{Cu}$ -foil.

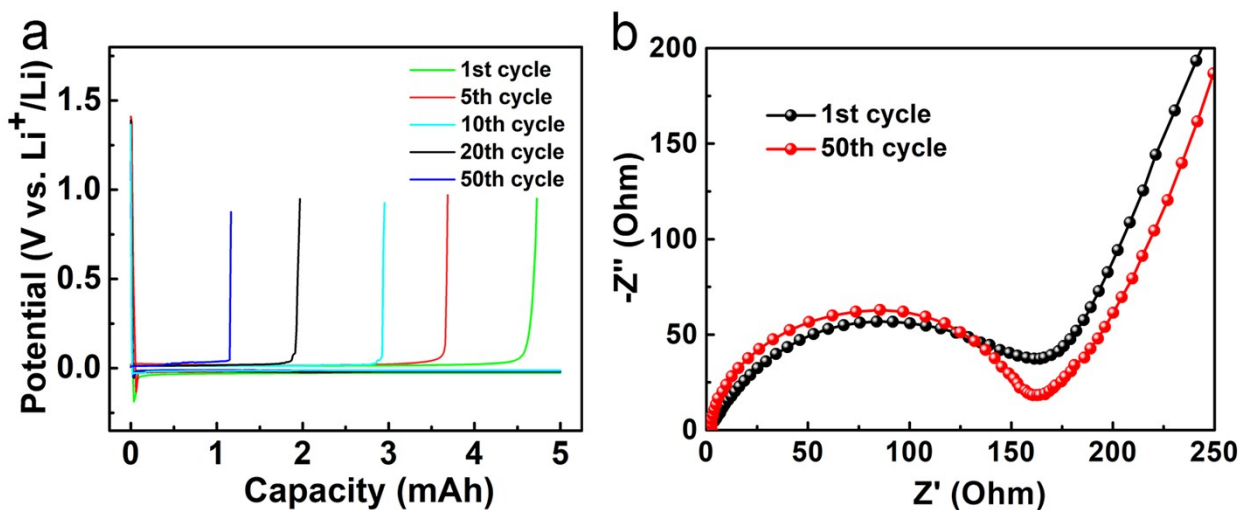


Fig. S4. (a) Voltage profiles of Li plating/stripping on/from planar Cu-foil at a current density of 5 mA cm⁻² with an areal capacity of 5 mAh cm⁻² after different cycles. (b) EIS plots of Ni₃(HITP)₂@Cu-foil at different cycles.

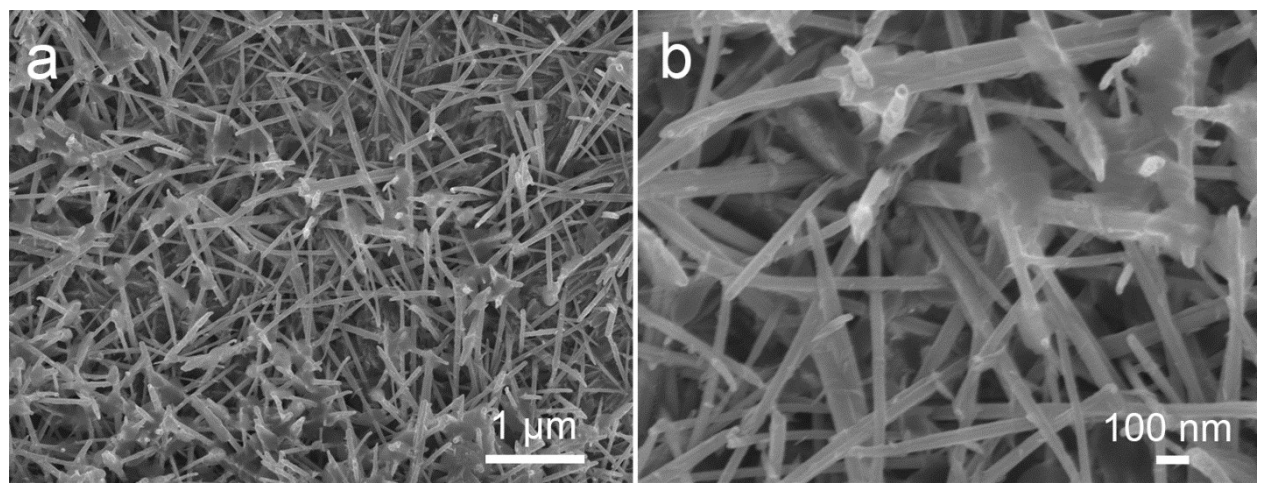


Fig. S5. SEM images of lithium metal deposited on the planar Cu-foil current collector under (a) low magnification and (b) high magnification.

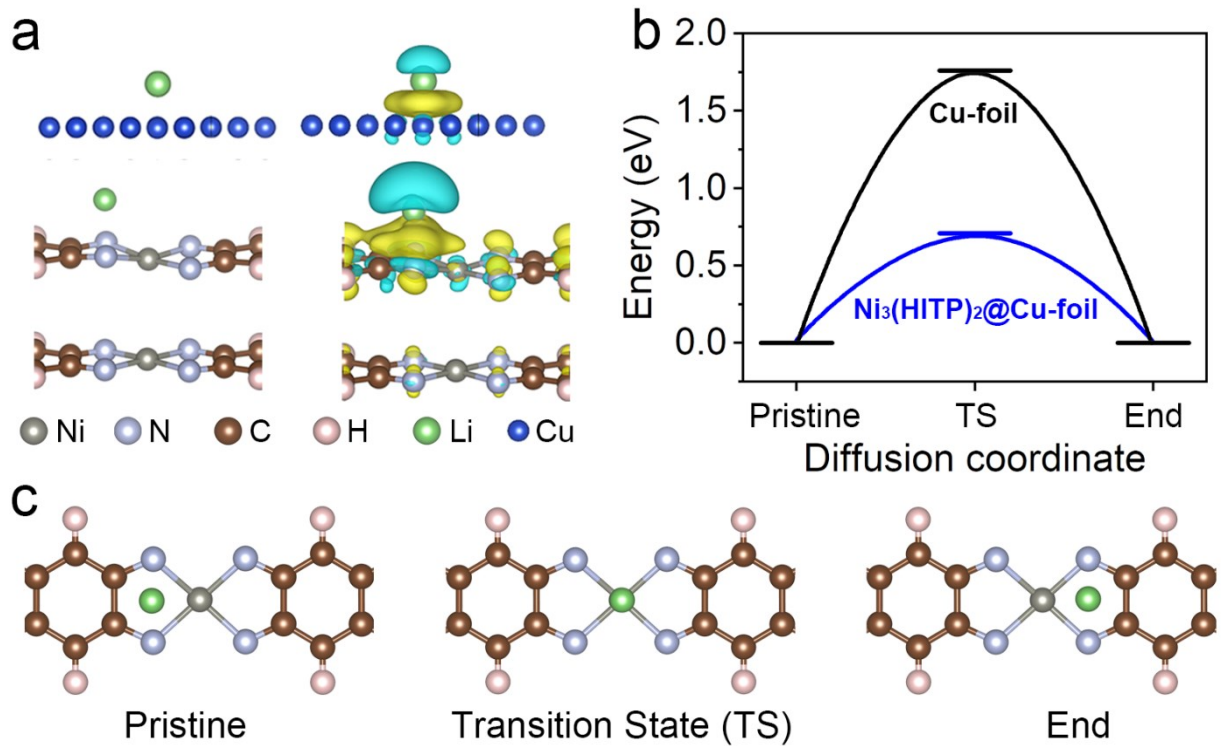


Fig. S6. a) Geometric configuration and corresponding charge density differences of a Li atom on the Cu-foil and $\text{Ni}_3(\text{HITP})_2$ @Cu-foil (the yellow and cyan regions represent positive and negative densities respectively. The isovalue for the charge density was taken as $\pm 0.002 \text{ e } \text{\AA}^{-3}$). b) A comparison of the diffusion barriers on Cu (111) and $\text{Ni}_3(\text{HITP})_2$. c) The diffusion pathway of Li atoms through the $\text{Ni}_3(\text{HITP})_2$ layers.

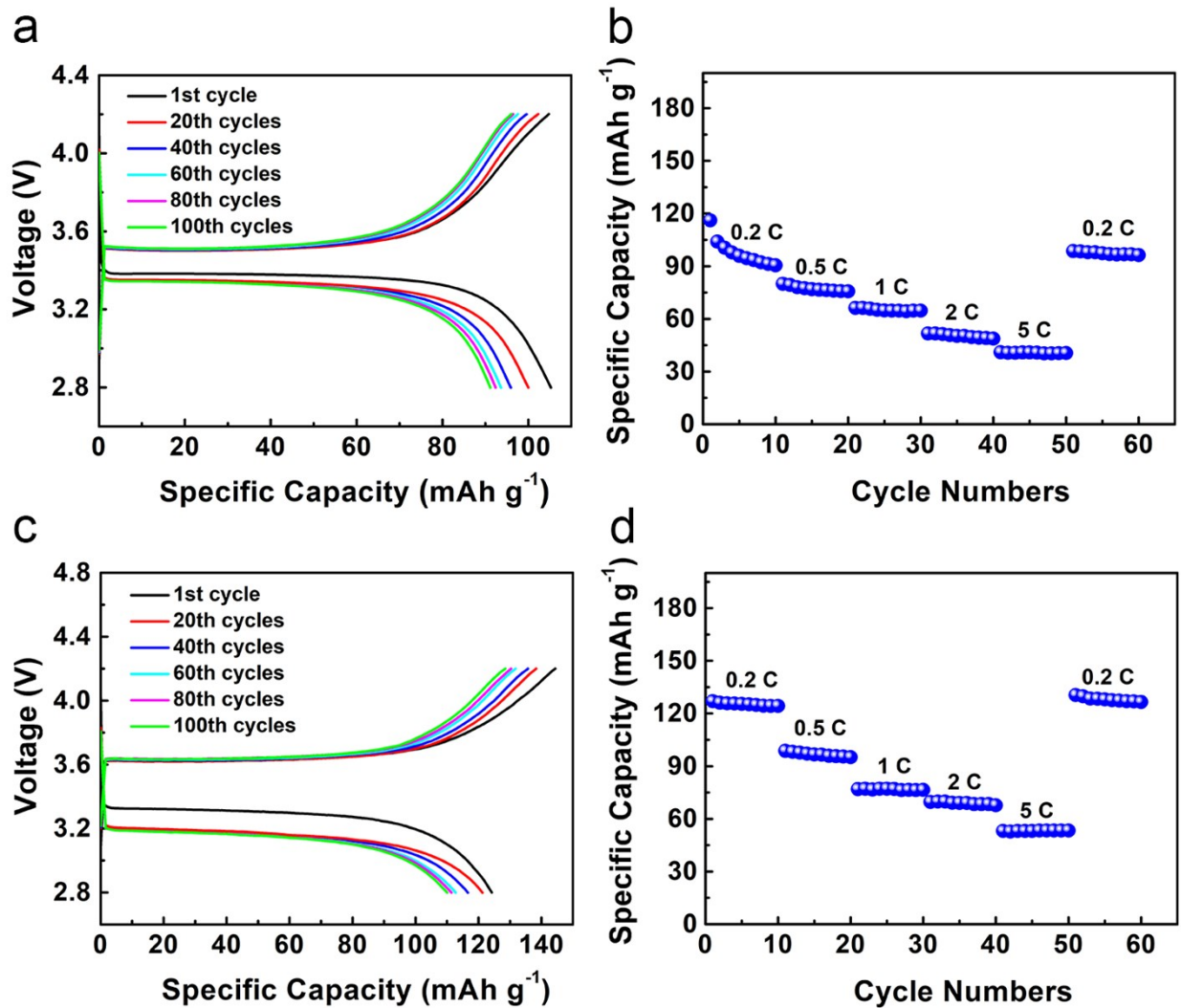


Fig. S7. (a) Voltage profiles and (b) rate capability of the $\text{Li}/\text{Ni}_3(\text{HITP})_2@\text{Cu}\text{-foil}|\text{LFP}$ cells with LFP capacity of 1.5 mAh cm^{-2} . (c) Voltage profiles and (d) rate capability of the $\text{Li}/\text{Ni}_3(\text{HITP})_2@\text{Cu}\text{-foil}|\text{LFP}$ cells with LFP capacity of 2.4 mAh cm^{-2} .